JAMA Ophthalmology | Original Investigation

Serial Combined Wide-Field Optical Coherence Tomography Maps for Detection of Early Glaucomatous Structural Progression

Won June Lee, MD; Tai Jun Kim, MD; Young Kook Kim, MD; Jin Wook Jeoung, MD, PhD; Ki Ho Park, MD, PhD

IMPORTANCE Both parapapillary and macular areas are important in determining the progression of early glaucoma. However, no attempt has been made to assess the progression of glaucoma in images that combine the 2 areas.

OBJECTIVE To evaluate the potential usefulness of serial analysis of combined wide-field optical coherence tomography (OCT) maps for detection of structural progression in patients with early glaucoma.

DESIGN, SETTING, AND PARTICIPANTS Retrospective observational study. Patients with early primary open-angle glaucoma with a minimum of 3-year follow-up involving serial spectral-domain OCT measurement were analyzed. Patients were divided into a nonprogressor group (n = 47) and a progressor group (n = 47) on the basis of serial stereo disc photography and red-free photography. Serial combined wide-field OCT maps integrating parapapillary retinal nerve fiber layer (RNFL) and macular ganglion cell–inner plexiform layer (GCIPL) maps were generated with the embedded software of serial spectral-domain OCT. Glaucoma specialists then assessed the structural progression detection ability of those serial wide-field OCT maps for early glaucomatous eyes and compared their sensitivity with those of RNFL and GCIPL guided progression analyses (GPAs).

MAIN OUTCOMES AND MEASURES The diagnostic ability of the serial wide-field OCT maps for early glaucomatous structural progression.

RESULTS Ninety-four patients (mean [SD] age, 51.4 [12.3] years; 48 [51.1%] women; all Korean) were included. The serial wide-field OCT map analysis showed good agreement for detection of structural progression between the 2 glaucoma graders (wide-field OCT thickness map: $\kappa = 0.649$; wide-field OCT deviation map: $\kappa = 0.833$). These maps showed early glaucomatous structural progression detection abilities comparable with those of RNFL and GCIPL GPAs (sensitivities of wide-field OCT thickness map, wide-field OCT deviation map, RNFL GPA, and GCIPL GPA = 63.8%, 83.0%, 83.0%, and 66.0%, respectively, all $P > .05$; specificities of wide-field OCT thickness map, wide-field OCT deviation map, RNFL GPA, and GCIPL GPA = 93.6%, 95.7%, 84.8%, and 93.6%, respectively, all $P > .05$).

CONCLUSIONS AND RELEVANCE The serial combined wide-field OCT maps integrating RNFL and GCIPL maps performed well in detecting structural progression in early glaucomatous eyes. Confirmation in an independent prospective study might provide greater confidence in this conclusion.

JAMA Ophthalmol. 2018;136(10):1121-1127. doi:10.1001/jamaophthalmol.2018.3160
Published online July 26, 2018.

Supplemental content

Author Affiliations: Department of Ophthalmology, Hanyang University Hospital, Seoul, Korea (Lee); Department of Ophthalmology, Hanyang University College of Medicine, Seoul, Korea (Lee); SNU Seoul Eye Clinic, Seoul, Korea (T. J. Kim); Department of Ophthalmology, Seoul National University Hospital, Seoul, Korea (Y. K. Kim, Jeoung, Park); Department of Ophthalmology, Seoul National University College of Medicine, Seoul, Korea (Y. K. Kim, Jeoung, Park).

Corresponding Author: Ki Ho Park, MD, PhD, Department of Ophthalmology, Seoul National University Hospital, Seoul National University College of Medicine, 101 Daehak-ro, Jongno-gu, Seoul 03080, Korea (kihopark@snu.ac.kr).

Evaluation of structural progression is essential to the overall treatment of patients with glaucoma and the management of their disease. For monitoring of glaucoma and detection of its structural progression, especially in the early stage, optical coherence tomography (OCT) has been widely used.[1-4] Classically, assessment of progressive changes in the optic disc and retinal nerve fiber layer (RNFL) is integral to evaluation of structural progression.[3] During the past few years, the value to glaucoma diagnosis of assessing the macular inner retinal structure, including the ganglion cell-inner plexiform layer (GCIPL), has been recognized and emphasized in many studies and reports. Indeed, those reports have demonstrated GCIPL parameters' comparable or better glaucoma progression detection and diagnostic performances compared with those of RNFL parameters.[5-9] Accordingly, many commercially available OCTs have provided glaucoma progression evaluation software (eg, Cirrus HD-OCT guided progression analysis [GPA] software[2,10]) based not only on RNFL but also GCIPL parameters.

Recently, many studies have attempted to integrate the RNFL and GCIPL diagnostic parameters and to determine their spatial relations. Wide-field OCT scanning with swept-source OCT (SS-OCT) technology also has been introduced and used in early glaucoma diagnosis. However, no studies using serial combined wide-field OCT maps integrating RNFL and GCIPL maps for determination of early glaucomatous structural progression have been reported to date and to our knowledge. The purpose of the present study was to evaluate the utility of the serial analysis and the diagnostic performance of wide-field OCT maps for detection of early glaucomatous structural progression, as clinically confirmed by stereo disc photographs and red-free photographs.

Key Points

Question Is serial analysis of combined wide-field optical coherence tomography maps integrating retinal nerve fiber layer and ganglion cell–inner plexiform layer maps useful in detecting structural progression in patients with early glaucoma?

Findings In this observational imaging study, the serial wide-field optical coherence tomography maps showed early glaucomatous structural progression detection abilities comparable with those of an embedded analysis software.

Meaning The serial combined wide-field optical coherence tomography maps performed well in detecting structural progression in early glaucomatous eyes, but confirmation in an independent prospective study might provide greater confidence in this conclusion.

Methods

This study was approved by the institutional review board of Seoul National University Hospital. All patients provided written informed consent. The study design followed the tenets of the Declaration of Helsinki[11] for biomedical research.

Participants

For this observational study, we enrolled 94 patients with early open-angle glaucoma (OAG) at the Department of Ophthalmology of Seoul National University Hospital from October 2012 to November 2017. Analyses began in December 2017. The study individuals were participants in the Macular Ganglion Cell Imaging Study, an ongoing prospective study designed in 2011. All participants underwent a complete ophthalmologic examination, including visual acuity testing, manifest refraction assessment, slitlamp examination, intraocular pressure measurements using Goldmann applanation tonometry, gonioscopy, dilated fundus examination, stereo disc photography and red-free RNFL photography (TRC-50IX; Topcon Corporation), Swedish interactive thresholding algorithm 30-2 perimetry (Humphrey Field Analyzer II; Carl Zeiss Meditec), and Cirrus HD-OCT (Carl Zeiss Meditec, Inc). Both eyes were imaged by Cirrus HD-OCT and examined by standard automated perimetry every 6 to 12 months for at least 36 months.

Patients with OAG were identified by the presence of a characteristic optic disc (ie, localized or diffuse neuroretinal rim thinning, increased cupping or cup-disc ratio difference >0.2 between the eyes) on stereo disc photography and the presence of RNFL defect on red-free fundus imaging, regardless of the presence or absence of glaucomatous visual field (VF) defects and an open angle confirmed by gonioscopic examination. Glaucomatous VF defects were defined as (1) glaucoma hemifield test values outside the normal limits; (2) 3 or more abnormal points with a less than 5% probability of being normal, among which at least 1 point has a pattern deviation probability of less than 1%; and (3) a pattern standard deviation probability of less than 5%. Visual field defects were confirmed on 2 consecutive reliable tests (fixation loss rate ≤20%, false-positive and false-negative error rates ≤25%). Also, enrolled patients with OAG all had a mean deviation of more than −6 dB or preperimetric glaucoma without glaucomatous VF defects.

The inclusion criteria were (1) unilateral or bilateral OAG, both eyes having a mean deviation of at least −6 dB on VF testing; (2) clinically confirmed structural progression during the follow-up period; and (3) follow-up examination with at least 4 serial RNFL and GCIPL OCT measurements and standard automated perimetry for more than 36 months. Additionally, patients eligible for inclusion in the study had to have a best-corrected visual acuity of 20/40 or better, spherical equivalent refractive errors between +6.0 and −6.0 D, and cylinder correction less than 3.0 D. The exclusion criteria were a history of ophthalmic surgery (eg, glaucoma-filtering surgery), any other ocular disease that could interfere with visual function, any media opacity that would significantly interfere with acquisition of OCT images, and inability to obtain a high-quality OCT image (ie, signal strength <6). For cases in which both eyes met all of the eligibility criteria, 1 eye was randomly chosen as the study eye prior to the analyses.

Determination of Glaucomatous Structural Progression

Each patient's structural progression status was determined from changes on entire series of stereo disc photography and

Figure 1. Baseline Wide-Field Optical Coherence Tomography (OCT) Maps of an Early Glaucomatous Left Eye of a 53-Year-Old Man

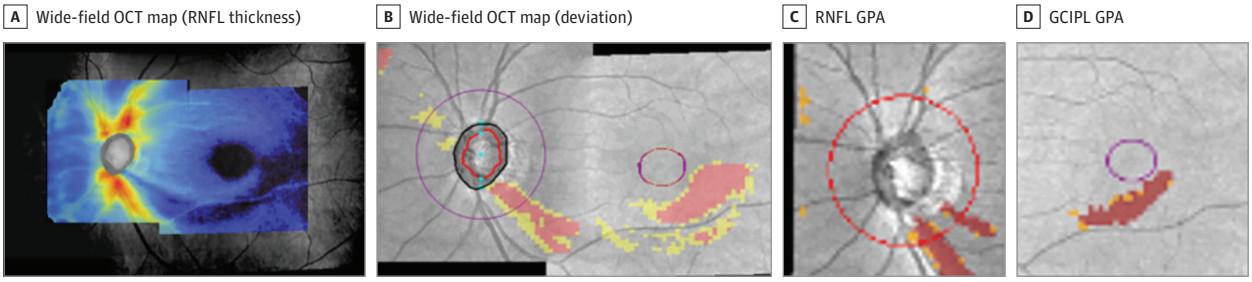

Combined wide-field OCT maps and guided progression analysis (GPA) results for retinal nerve fiber layer (RNFL) and ganglion cell–inner plexiform layer (GCIPL) of early glaucomatous eye. A full version of serial combined wide-field OCT maps and GPA results for RNFL and GCIPL is available in eFigure 1 in the Supplement. Structural progression on the serial wide-field OCT maps (RNFL thickness map, deviation map set) and in both RNFL and GCIPL GPAs was clear.

Figure 2. Baseline Wide-Field Optical Coherence Tomography (OCT) Maps of an Early Glaucomatous Right Eye of a 51-Year-Old Man

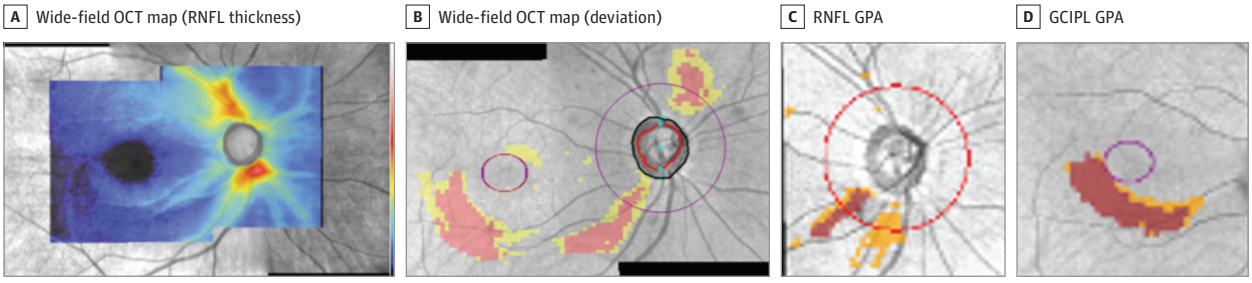

Combined wide-field OCT maps and guided progression analysis (GPA) results for retinal nerve fiber layer (RNFL) and ganglion cell–inner plexiform layer (GCIPL) of early glaucomatous eye. A full version of serial combined wide-field OCT maps and GPA results for RNFL and GCIPL is available in eFigure 2 in the Supplement. Widening of defects was clearly visible in both the parapapillary and macular area of the wide-field OCT deviation map. Structural progression was well detected in both the RNFL and GCIPL GPAs.

RNFL photography (nonprogressor vs progressor). Progressive optic disc changes (ie, focal or diffuse rim narrowing, neuroretinal rim notching, increased cup-disc ratio, adjacent vasculature position shift) were determined by comparison of entire serial stereo disc photographic images and regarded as indicative of glaucoma progression. Changes in RNFL defects were determined from entire serial RNFL photographs and defined as the appearance of a new defect or an increase in the width or depth of an existing defect. These changes were regarded as indicative of clinically confirmed structural progression.[12] Two observers (Y.K.K. and J.W.J.) masked to all other patient information independently evaluated all of the photographs. In cases of disagreement, a third glaucoma specialist (K.H.P.) served as an adjudicator.

Combined Wide-Field OCT Maps

The optic disc cube scan (200 × 200 pixels) and ganglion cell analysis protocol for macular cube scanning (6 × 6 mm^2, 200 × 200 pixels) were used for diagnosis of and follow-up on glaucoma. Detailed information on those procedures has been previously published.[13]

With the built-in analysis software (Cirrus HD-OCT software, version 10.0), combined wide-field OCT maps (Pano-Maps, CSA) were generated. Two maps (optic disc cube and macular cube) obtained on the same day were integrated into 1 image, and the data sets were montaged. The OCT en face images are registered to each other using the blood vessel crossings as features. The transformation derived from this was used to adjust the thickness maps and deviation maps for the purpose of presentation. The 2 scans were blended using an algorithm, which combined the 2 maps in the areas of overlap. Thereby, the combined wide-field RNFL thickness map and combined wide-field deviation map were obtained. For the deviation maps, if a pixel was deviated from either the optic disc cube or macular cube, it was shown as deviated on the wide-field OCT maps (**Figure 1**, **Figure 2**, and eFigures 1, 2, 3, and 4 in the Supplement).

Determination of Early Glaucomatous Structural Progression in Wide-Field OCT Maps

To evaluate structural progression using the serial wide-field OCT maps, 2 sets of serial wide-field OCT thickness maps and wide-field OCT deviation maps for each patient were prepared (Figure 1, Figure 2, and eFigures 1, 2, 3, and 4 in the Supplement). Structural progression on the serial wide-field OCT thickness maps was defined as the appearance of a new RNFL defect or an increase in the width or depth of an existing defect. Structural progression on the serial wide-field OCT deviation maps was defined as the appearance of a new RNFL defect (deviated pixels) or an increase in the width of an

Table 1. Clinical Demographic Characteristics of Patients With Early Glaucoma

Variable[a,b]	Nonprogressor Group (n = 47)	Progressor Group (n = 47)
Age, y	51.3 (12.0)	51.5 (12.7)
Men, No. (%)	25 (53.2)	21 (44.7)
Diabetes, No. (%)	5 (10.6)	5 (10.6)
Hypertension, No. (%)	8 (17.0)	8 (17.0)
OCT scan number	5.3 (0.9)	5.5 (0.9)
Follow-up period, mo	57.1 (6.5)	56.1 (7.1)
IOP, mm Hg	14.4 (4.2)	14.0 (2.2)
No. of medications[c]	0.8 (0.7)	0.6 (0.5)
CCT, µm	552.0 (31.7)	541.2 (29.1)
Visual field parameters		
MD, dB	−1.9 (2.5)	−1.9 (2.1)
PSD, dB	4.4 (3.4)	4.2 (3.1)
VFI, No. (%)	95.1 (6.4)	95.4 (5.2)
RNFL thickness, µm	85.5 (9.5)	82.6 (9.9)
GCIPL thickness, µm	76.0 (6.4)	75.4 (5.2)
Disc hemorrhage during follow-up period, No. (%)[c]	2 (4.3)	24 (51.1)

Abbreviations: CCT, central corneal thickness; GCIPL, ganglion cell-inner plexiform layer; IOP, intraocular pressure; MD, mean deviation; OCT, optical coherence tomography; PSD, pattern standard deviation; RNFL, retinal nerve fiber layer; VFI, visual field index.

[a] Data are reported as mean (SD) unless otherwise stated.

[b] Comparisons were performed with the χ^2 test for categorical variables and the independent *t* test for continuous variables.

[c] The differences between 2 groups were statistically significant with *P* value less than .05.

existing defect (deviated pixels). Two observers (W.J.L. and T.J.K.) masked to all other patient information independently evaluated all of the serial image sets. In cases of disagreement, a third glaucoma specialist (K.H.P.) served as an adjudicator.

The Cirrus HD-OCT GPA (version 10.0) provided event and trend analyses for detection of progressive thinning of the parapapillary RNFL and macular GCIPL. The method has been described in detail elsewhere.[14] Structural progression, as detected by OCT GPAs during follow-up, was defined as likely progression in the event analysis (RNFL change map and summary of parameters or GCIPL change map and summary of parameters), and the same changes were observed at the latest follow-up visit.

Statistical Analyses

All of the statistical tests were performed using PASW Statistics, version 18 (SPSS). To evaluate the interobserver-agreement reliability for determination of structural progression using serial wide-field OCT maps, κ coefficients were calculated. To compare the characteristics, including the changing rates of OCT parameters, χ^2 test for categorical variables and the independent *t* test for continuous variables were used. To assess the abilities of each categorical variables such as serial wide-field OCT maps to distinguish participants with progressor from nonprogressor, sensitivities and specificities were tested. The McNemar test was used to compare the sensitivities and specificities of the different OCT methods (wide-field OCT maps and GPAs) for detection of structural progression. The values were recorded in the form of the mean (SD). *P* values less than .05 were considered statistically significant.

Results

The study involved 94 early OAG eyes meeting the inclusion criteria. Of these, 47 eyes (50%) were classified as nonprogressors and 47 eyes (50%) were classified as progressor on the basis of serial stereo disc photography and red-free fundus photography (clinically confirmed structural progression).

Clinical Demographics

All 94 patients with early OAG (48 women [51.1%]) were Korean, and the mean (SD) age was 51.4 (12.3) years. **Table 1** shows the clinical demographics of all patients at the time of enrollment. The mean (SD) number of OCT scans was 5.4 (0.9), and the mean (SD) follow-up period was 56.6 (6.8) months. Nonprogressors and progressors showed no significant differences in terms of age (mean [SD], 51.3 [12.0] vs 51.5 [12.7] years; *P* = .96), intraocular pressure, VF indices, baseline RNFL thickness (mean [SD], 85.5 [9.5] vs 82.6 [9.9] µm; *P* = .14), and GCIPL thickness (mean [SD], 76.0 [6.4] vs 75.4 [5.2] µm; *P* = .61). The mean number of OCT scans (mean [SD], 5.3 [0.9] vs 5.5 [0.9]; *P* = .15) and the follow-up periods (mean [SD], 57.1 [6.5] vs 56.1 [7.1] months; *P* > .46) were similar between the groups. Among the 47 eyes showing clinically confirmed structural progression, 24 (51.1%) presented disc hemorrhage during the follow-up period.

Guided Progression Analysis

Table 2 shows the GPA results of both the RNFL and GCIPL analyses. The rates of RNFL and GCIPL thinning were significantly faster in progressors than in nonprogressors globally (RNFL: mean [SD], −1.65 [0.94] vs −0.61 [0.78] µm/y; *P* < .001) (GCPIL: mean [SD], −0.91 [0.58] vs −0.27 [0.33] µm/y; *P* < .001) in the superior (RNFL: mean [SD], −2.03 [1.36] vs −0.90 [0.76] µm/y; *P* < .001) (GCPIL: mean [SD], −0.72 [0.76] vs −0.18 [0.37] µm/y; *P* < .001) and inferior hemi-retinas (RNFL: mean [SD], −2.91 [2.18] vs −1.23 [1.15] µm/y; *P* < .001) (GCPIL: mean [SD], −1.10 [0.82] vs −0.34 [0.39] µm/y; *P* < .001). The RNFL and GCIPL GPA detected a significant difference in progression between progressor and nonprogressor groups (RNFL: 39 [83.0%] vs 7 [15.2%]; *P* < .001) (GCIPL: 31 (66.0%) vs 3 (6.4%); *P* < .001).

Sensitivities and Specificities of Combined Wide-Field OCT Maps for Detection of Clinically Confirmed Structural Progression

The 2 graders showed good overall agreement in determining whether structural progression had been detected (wide-field OCT thickness map: κ = 0.649, *P* < .001; wide-field OCT deviation map: κ = 0.833, *P* < .001). The sensitivities and specificities of the combined wide-field OCT maps and GPAs are presented in **Table 3**. The combined wide-field OCT maps

Table 2. Guided Progression Analysis Results in Patients With Nonprogressing and Progressing Glaucoma

Variable[a,b]	Nonprogressor Group (n = 47)	Progressor Group (n = 47)	Difference (95% CI)	*P* Value
RNFL GPA				
Structural progression on GPA, No. (%)	7 (15.2)	39 (83.0)	67.8 (48.4-80.7)	<.001
Mean RNFL thinning rate, µm/y	−0.61 (0.78)	−1.65 (0.94)	1.03 (0.67-1.39)	<.001
Superior RNFL thinning rate, µm/y	−0.90 (1.39)	−2.03 (1.36)	1.12 (0.56-1.69)	<.001
Inferior RNFL thinning rate, µm/y	−1.23 (1.15)	−2.91 (2.18)	1.68 (0.95-2.40)	<.001
GCIPL GPA				
Structural progression on GPA, No. (%)	3 (6.4)	31 (66.0)	59.6 (40.7-73.7)	<.001
Mean GCIPL thinning rate, µm/y	−0.27 (0.33)	−0.91 (0.58)	0.64 (0.45-0.84)	<.001
Superior GCIPL thinning rate, µm/y	−0.18 (0.37)	−0.72 (0.76)	0.54 (0.29-0.78)	<.001
Inferior GCIPL thinning rate, µm/y	−0.34 (0.39)	−1.10 (0.82)	0.76 (0.49-1.03)	<.001
Humphrey visual field GPA				
Functional progression on GPA,[c] No. (%)	6 (12.8)	15 (31.9)	19.1 (0.85-35.3)	.03
Visual field index decreasing rate, %/y	−0.16 (0.64)	−0.65 (1.08)	0.49 (0.11-0.87)	.02

Abbreviations: GCIPL, ganglion cell–inner plexiform layer; GPA, guided progression analysis; RNFL, retinal nerve fiber layer.

[a] Data are reported as mean (SD) unless otherwise indicated.

[b] Comparisons were performed with the χ^2 test for categorical variables and the independent *t* test for continuous variables.

[c] Functional progression was confirmed when at least 3 test points were flagged as having deteriorated significantly at the same test point locations in 3 consecutive fields (the software classifies visual field progression as likely progression). These changes also had to have been observed at the final visit.

Table 3. Comparison of Sensitivities and Specificities for Detection of Clinically Confirmed Structural Progression in Early Glaucoma[a]

Variable	Sensitivity, No. (%)	95% CI	*P* Value 1[b]	*P* Value 2[c]	*P* Value 3[d]	*P* Value 4[e]	Specificity, No. (%)	95% CI	*P* Value 1[b]	*P* Value 2[c]	*P* Value 3[d]	*P* Value 4[e]
RNFL GPA	39 (83.0)	69.2-92.4	NA	.08	.06	>.99	39 (84.8)	71.1-93.7	NA	.22	.34	.18
GCIPL GPA	31 (66.0)	50.7-79.1	.08	NA	>.99	.08	44 (93.6)	82.5-98.7	.22	NA	>.99	>.99
Wide-field OCT map (thickness)	30 (63.8)	48.5-77.3	.06	.06	NA	.06	44 (93.6)	82.5-98.7	.34	>.99	NA	>.99
Wide-field OCT map (deviation)	39 (83.0)	69.2-92.4	>.99	.08	.06	NA	45 (95.7)	85.5-99.5	.18	>.99	>.99	NA

Abbreviations: GCIPL, ganglion cell–inner plexiform layer; GPA, guided progression analysis; NA, not applicable; OCT, optical coherence tomography; RNFL, retinal nerve fiber layer.

[a] No mathematical correction was made for multiple comparisons.

[b] *P* value 1 compared with RNFL GPA result (McNemar test).

[c] *P* value 2 compared with GCIPL GPA result (McNemar test).

[d] *P* value 3 compared with wide-field OCT map thickness result (McNemar test).

[e] *P* value 4 compared with wide-field OCT map deviation result (McNemar test).

showed sensitivities and specificities for detection of structural progression in early glaucoma comparable with those of the RNFL and GCIPL GPAs (sensitivities: wide-field OCT thickness map, wide-field OCT deviation map, RNFL GPA, and GCIPL GPA = 63.8%, 83.0%, 83.0%, and 66.0%, respectively; all $P > .05$; specificities: wide-field OCT thickness map, wide-field OCT deviation map, RNFL GPA, and GCIPL GPA = 93.6%, 95.7%, 84.8%, and 93.6%, respectively; all $P > .05$).

Discussion

Efforts to evaluate glaucomatous structural progression, especially in the early stage of glaucoma, have been redoubled in recent years.[15-17] Also, the evaluation approach has evolved, becoming more comprehensive in including the optic disc and macular area.[18-23] Our study demonstrated, as confirmed by stereo disc photography and/or red-free fundus photography, that serial combined wide-field OCT maps show detecting ability comparable with RNFL and GCIPL GPA software in determining structural progression in eyes with early OAG. To our knowledge, this is the first study to apply commercially available combined wide-field OCT maps for evaluation of structural progression.

Recently, a few studies that evaluated glaucomatous structural progression with reference to the inner macular area including the GCIPL and RNFL have been published.[13,14,24,25] The macular GCIPL thinning rates of glaucomatous eyes were faster than those of normal healthy eyes[24] and were significantly faster for patients with glaucoma with progression than for those without progression.[13] Commercially available GCIPL GPA provides a new approach to the evaluation of structural progression, one that may be more useful than RNFL GPA for detection of progression in advanced glaucoma.[14]

Additionally to these studies, attempts have been made to integrate parapapillary RNFL and macular GCIPL in the evaluation of glaucomatous eyes. In 2017, Hood[20] hypothesized that early glaucomatous damage involves the macular area and that glaucomatous macular damage typically is associated with local RNFL thinning in a narrow region of the disc that they called the macular vulnerability zone. The same research group recently developed a probability map (ie, the study by Hood[20]) using SS-OCT technology with its wide-field scan protocol (12 × 9 mm) that makes possible the direct comparison of local retinal ganglion cell and RNFL loss with local loss in VF sensitivities.[18,20,21,26-28] However, their OCT device was a prototype and not commercially available, and their software also was under development; moreover, they did not evaluate pro-

gression with serial OCT maps. After wide-field SS-OCT scanning and an SS-OCT probability map became commercially available, the diagnostic performance of wide-field SS-OCT RNFL maps for early glaucoma[29] and of the study by Hood[20] for prediction of future VF changes in preperimetric glaucoma patients,[30] respectively, were evaluated. However, structural progression was not evaluated in either study.

A wide-field OCT map (Cirrus) prototype recently was introduced in a study evaluating the effect of fovea-disc-angle axis adjustment, but that study did not evaluate structural progression either.[31] More recently, our group introduced an integrated deviation map merged by superimposition of parapapillary RNFL and macular GCIPL deviation maps (from a Cirrus HD-OCT) onto RNFL photography as aligned by a raster graphics editor (Adobe Photoshop) software based on vascular landmarks.[22,23] The method used in those studies was similar to the principle of wide-field OCT map operation. In those studies, we classified early glaucomatous changes according to the topographic association between parapapillary RNFL and macular GCIPL deviation maps[23] and observed longitudinal progression patterns among the classified subgroups.[22] However, we evaluated progression only with 2 integrated deviation maps (the initial map and the final map introduced 3 years later), and we performed no automated integration by algorithm (ie, by wide-field OCT maps) or serial comparisons.

Combined wide-field OCT maps have a number of advantages for evaluation of glaucomatous structural progression. First, structural progression can be interpreted comprehensively in both the parapapillary and macular areas in 1 single image. Note too that as the hardware and software are developed over time, it will be possible to capture this wide area at once and perform wide-field GPA for automatic determination of progression. Second, various progression patterns of glaucomatous change can be observed and investigated. In the present study, as in an aforementioned study,[22] there were some cases showing infero-inferior RNFL defect with inferior macular GCIPL defect that were not directly connected on the deviation map at the baseline. As the disease progressed, RNFL thinning in the macular vulnerability zone developed, and the defects on the deviation maps were connected with each other (Figure 1 and Figure 2). In other patterns showing RNFL defect in the macular vulnerability zone with corresponding macular GCIPL defect at the baseline, the widening of defects were progressed in both the parapapillary and macular areas and connected with each other (eFigures 3 and 4 in the Supplement). Also, there was another pattern showing newly developed defects rather than preexisting ones, in which cases those new defects were well visible on the combined wide-field OCT maps (eFigure 4 in the Supplement). Although we could not classify the progression patterns precisely in this study owing to the small sample size, our serial combined wide-field OCT maps analysis certainly will facilitate progression-pattern classification in a future study. The third advantage of wide-field OCT maps for evaluation of glaucomatous structural progression is that they can provide more objective information for more accurate determination of structural progression. Whereas stereo disc photography and red-free photography have indeed been the criterion standard for determination of structural progression, it is sometimes very difficult, with conventional red-free photography, to evaluate deepening or widening of RNFL defects (because it is affected by photograph quality and a patient's pigmentation status).[32] Combined wide-field OCT maps visualized by color coding with an objective digitalized database or deviation-from-normative database can provide results that are more objective for evaluation of structural progression. In this regard, the wide-field OCT deviation map, compared with the wide-field OCT thickness map, might offer the chief benefit, as it is more objective and can visualize quantitative analysis results.

Limitations

This new visualizing technology has some limitations. First, in the process of combining the 2 OCT maps, errors such as misalignment of the fovea-disc-angle axis or a too-short distance between the fovea and disc can be incurred, which errors, because manual modification is impossible, interfere with the analysis. In the present study therefore, we excluded such error images from our analysis. We analyzed a total of 472 wide-field OCT map images, of which 22 (4.7%) had problems as described above. Second, combining the wide-field OCT map images and serializing them for analysis is time consuming. It is expected that these limitations will be overcome once newer technology becomes available in the near future.

Our study has several weaknesses. First of all, the small sample size might be the major limitation of this study. Because we performed this study based on a previous cohort that had been evaluating glaucoma progression, the proportion of progressors were relatively high. Independent prospective study with larger samples might provide greater information, especially in cases showing discrepancy between RNFL and GCIPL GPA. Second, we determined whether structural progression on combined wide-field OCT maps was visible or not, which depends on graders' judgment based on a qualitative approach. Although we performed the analyses in the masked fashion and evaluated the interobserver agreement with statistical methods, the objectivity of those determinations could be challenged. Third, we enrolled only patients with early-stage glaucoma for this imaging study because RNFL or GCIPL defects are well visible on thickness and deviation maps only in such cases. Indeed, by our quantitative approach, patients with severe myopia or advanced-stage glaucoma with diffusely thinned retinal layers cannot be evaluated. Fourth, because the reference standard of progressive changes relied on detecting change on stereo disc photographs and red-free RNFL photographs, GCIPL may not be as good at detecting glaucoma progression. Fifth, the number of OCT images acquired was limited and this may be insufficient to confidently detect progression. Thus, further studies acquiring more OCT images may be required to evaluate the structural progression.

Conclusions

Serial combined wide-field OCT maps integrating RNFL and GCIPL OCT maps performed well in detecting structural progression in early glaucomatous eyes. Serial analysis with these maps facilitates effective visualization and objective assessment of structural progression.

ARTICLE INFORMATION

Accepted for Publication: May 31, 2018.

Published Online: July 26, 2018. doi:10.1001/jamaophthalmol.2018.3160

Author Contributions: Dr Park had full access to all of the data in the study and takes responsibility for the integrity of the data and the accuracy of the data analysis.
Concept and design: Lee, Jeoung, Park.
Acquisition, analysis, or interpretation of data: All authors.
Drafting of the manuscript: Lee, T. Kim.
Critical revision of the manuscript for important intellectual content: Lee, Y. Kim, Jeoung, Park.
Statistical analysis: Lee, T. Kim, Jeoung.
Administrative, technical, or material support: Lee, T. Kim, Jeoung, Park.
Supervision: Lee, Y. Kim, Jeoung, Park.

Conflict of Interest Disclosures: All authors have completed and submitted the ICMJE Form for Disclosure of Potential Conflicts of Interest and none were reported.

Additional Contributions: We thank Eunwoo Nam, PhD, in the Biostatistical Consulting and Research Lab, Hanyang University, Seoul, Korea for assistance with statistical consultation during the revision. Dr Nam was not compensated.

REFERENCES

1. Lee EJ, Kim TW, Weinreb RN, Park KH, Kim SH, Kim DM. Trend-based analysis of retinal nerve fiber layer thickness measured by optical coherence tomography in eyes with localized nerve fiber layer defects. *Invest Ophthalmol Vis Sci*. 2011;52(2):1138-1144. doi:10.1167/iovs.10-5975

2. Leung CK. Diagnosing glaucoma progression with optical coherence tomography. *Curr Opin Ophthalmol*. 2014;25(2):104-111. doi:10.1097/ICU.0000000000000024

3. Leung CK, Cheung CY, Weinreb RN, et al. Evaluation of retinal nerve fiber layer progression in glaucoma: a study on optical coherence tomography guided progression analysis. *Invest Ophthalmol Vis Sci*. 2010;51(1):217-222. doi:10.1167/iovs.09-3468

4. Wollstein G, Schuman JS, Price LL, et al. Optical coherence tomography longitudinal evaluation of retinal nerve fiber layer thickness in glaucoma. *Arch Ophthalmol*. 2005;123(4):464-470. doi:10.1001/archopht.123.4.464

5. Jeoung JW, Choi YJ, Park KH, Kim DM. Macular ganglion cell imaging study: glaucoma diagnostic accuracy of spectral-domain optical coherence tomography. *Invest Ophthalmol Vis Sci*. 2013;54(7):4422-4429. doi:10.1167/iovs.12-11273

6. Mwanza JC, Durbin MK, Budenz DL, et al. Glaucoma diagnostic accuracy of ganglion cell-inner plexiform layer thickness: comparison with nerve fiber layer and optic nerve head. *Ophthalmology*. 2012;119(6):1151-1158. doi:10.1016/j.ophtha.2011.12.014

7. Jeong JH, Choi YJ, Park KH, Kim DM, Jeoung JW. Macular ganglion cell imaging study: covariate effects on the spectral domain optical coherence tomography for glaucoma diagnosis. *PLoS One*. 2016;11(8):e0160448. doi:10.1371/journal.pone.0160448

8. Lee SY, Jeoung JW, Park KH, Kim DM. Macular ganglion cell imaging study: interocular symmetry of ganglion cell-inner plexiform layer thickness in normal healthy eyes. *Am J Ophthalmol*. 2015;159(2):315-23.e2. doi:10.1016/j.ajo.2014.10.032

9. Kim KE, Park KH. Macular imaging by optical coherence tomography in the diagnosis and management of glaucoma. *Br J Ophthalmol*. 2018;102(6):718-724. doi:10.1136/bjophthalmol-2017-310869

10. Leung CK, Yu M, Weinreb RN, Lai G, Xu G, Lam DS. Retinal nerve fiber layer imaging with spectral-domain optical coherence tomography: patterns of retinal nerve fiber layer progression. *Ophthalmology*. 2012;119(9):1858-1866. doi:10.1016/j.ophtha.2012.03.044

11. World Medical Association. World Medical Association Declaration of Helsinki: ethical principles for medical research involving human subjects. *JAMA*. 2013;310(20):2191-2194. doi:10.1001/jama.2013.281053.

12. Suh MH, Kim DM, Kim YK, Kim TW, Park KH. Patterns of progression of localized retinal nerve fibre layer defect on red-free fundus photographs in normal-tension glaucoma. *Eye (Lond)*. 2010;24(5):857-863. doi:10.1038/eye.2009.209

13. Lee WJ, Kim YK, Park KH, Jeoung JW. Trend-based analysis of ganglion cell-inner plexiform layer thickness changes on optical coherence tomography in glaucoma progression. *Ophthalmology*. 2017;124(9):1383-1391. doi:10.1016/j.ophtha.2017.03.013

14. Shin JW, Sung KR, Lee GC, Durbin MK, Cheng D. Ganglion cell-inner plexiform layer change detected by optical coherence tomography indicates progression in advanced glaucoma. *Ophthalmology*. 2017;124(10):1466-1474. doi:10.1016/j.ophtha.2017.04.023

15. Sung KR, Sun JH, Na JH, Lee JY, Lee Y. Progression detection capability of macular thickness in advanced glaucomatous eyes. *Ophthalmology*. 2012;119(2):308-313. doi:10.1016/j.ophtha.2011.08.022

16. Na JH, Sung KR, Lee JR, et al. Detection of glaucomatous progression by spectral-domain optical coherence tomography. *Ophthalmology*. 2013;120(7):1388-1395. doi:10.1016/j.ophtha.2012.12.014

17. Medeiros FA, Zangwill LM, Alencar LM, et al. Detection of glaucoma progression with stratus OCT retinal nerve fiber layer, optic nerve head, and macular thickness measurements. *Invest Ophthalmol Vis Sci*. 2009;50(12):5741-5748. doi:10.1167/iovs.09-3715

18. Hood DC, Raza AS, de Moraes CG, Liebmann JM, Ritch R. Glaucomatous damage of the macula. *Prog Retin Eye Res*. 2013;32:1-21. doi:10.1016/j.preteyeres.2012.08.003

19. Kim KE, Park KH, Yoo BW, Jeoung JW, Kim DM, Kim HC. Topographic localization of macular retinal ganglion cell loss associated with localized peripapillary retinal nerve fiber layer defect. *Invest Ophthalmol Vis Sci*. 2014;55(6):3501-3508. doi:10.1167/iovs.14-13925

20. Hood DC. Improving our understanding, and detection, of glaucomatous damage: an approach based upon optical coherence tomography (OCT). *Prog Retin Eye Res*. 2017;57:46-75. doi:10.1016/j.preteyeres.2016.12.002

21. Hood DC, Raza AS. On improving the use of OCT imaging for detecting glaucomatous damage. *Br J Ophthalmol*. 2014;98(suppl 2):ii1-ii9. doi:10.1136/bjophthalmol-2014-305156

22. Kim YK, Ha A, Na KI, Kim HJ, Jeoung JW, Park KH. Temporal relation between macular ganglion cell-inner plexiform layer loss and peripapillary retinal nerve fiber layer loss in glaucoma. *Ophthalmology*. 2017;124(7):1056-1064. doi:10.1016/j.ophtha.2017.03.014

23. Kim YK, Jeoung JW, Park KH. Inferior macular damage in glaucoma: its relationship to retinal nerve fiber layer defect in macular vulnerability zone. *J Glaucoma*. 2017;26(2):126-132.

24. Hammel N, Belghith A, Weinreb RN, Medeiros FA, Mendoza N, Zangwill LM. Comparing the rates of retinal nerve fiber layer and ganglion cell-inner plexiform layer loss in healthy eyes and in glaucoma eyes. *Am J Ophthalmol*. 2017;178:38-50. doi:10.1016/j.ajo.2017.03.008

25. Lee WJ, Kim YK, Park KH, Jeoung JW. Evaluation of ganglion cell-inner plexiform layer thinning in eyes with optic disc hemorrhage: a trend-based progression analysis. *Invest Ophthalmol Vis Sci*. 2017;58(14):6449-6456. doi:10.1167/iovs.17-22547

26. Hood DC, De Cuir N, Blumberg DM, et al. A single wide-field OCT protocol can provide compelling information for the diagnosis of early glaucoma. *Transl Vis Sci Technol*. 2016;5(6):4. doi:10.1167/tvst.5.6.4

27. Hood DC, Fortune B, Mavrommatis MA, et al. Details of glaucomatous damage are better seen on OCT en face images than on oct retinal nerve fiber layer thickness maps. *Invest Ophthalmol Vis Sci*. 2015;56(11):6208-6216. doi:10.1167/iovs.15-17259

28. Hood DC, Raza AS. Method for comparing visual field defects to local RNFL and RGC damage seen on frequency domain OCT in patients with glaucoma. *Biomed Opt Express*. 2011;2(5):1097-1105. doi:10.1364/BOE.2.001097

29. Lee WJ, Na KI, Kim YK, Jeoung JW, Park KH. Diagnostic ability of wide-field retinal nerve fiber layer maps using swept-source optical coherence tomography for detection of preperimetric and early perimetric glaucoma. *J Glaucoma*. 2017;26(6):577-585. doi:10.1097/IJG.0000000000000662

30. Lee WJ, Kim YK, Jeoung JW, Park KH. Can probability maps of swept-source optical coherence tomography predict visual field changes in preperimetric glaucoma? *Invest Ophthalmol Vis Sci*. 2017;58(14):6257-6264. doi:10.1167/iovs.17-22697

31. Mwanza JC, Lee G, Budenz DL. Effect of adjusting retinal nerve fiber layer profile to fovea-disc angle axis on the thickness and glaucoma diagnostic performance. *Am J Ophthalmol*. 2016;161:12-21.e1, 2. doi:10.1016/j.ajo.2015.09.019

32. Hitchings RA, Poinoosawmy D, Poplar N, Sheth GP. Retinal nerve fibre layer photography in glaucomatous patients. *Eye*. 1987;1(5):621-625. doi:10.1038/eye.1987.96